Investigating streamflow response to future climate and land cover change scenarios in the Rio Grande Headwaters

Final Report, June 2022

Authors:

Katie E. Schneider[1*], Ashley Rust[2], Terri Hogue[1,2]

[1]*Hydrologic Science and Engineering, Colorado School of Mines*
[2]*Civil and Environmental Engineering, Colorado School of Mines*
[*]*A modified version of this report was included in Katie Schneider's dissertation submission in November 2021 and was submitted to the Journal of the American Water Resources Association in April 2022.*

1

Executive Summary

Like many forested and snow dominated catchments in the arid western U.S., Colorado's Rio Grande Headwaters (RGH) has experienced numerous land cover disruptions in recent decades. These land cover disturbances have occurred as stand-alone events ("single disturbances") and as events that overlap one another in space and time ("overlapping disturbances"). Severe drought in the early 2000s, widespread spruce beetle induced forest mortality (~2005-2011) and the West Fork Complex Fire of 2013 have raised concerns about streamflow resilience under future climate and land cover disturbance scenarios. This study was developed as a collaborative effort between the Colorado School of Mines and RGH stakeholders who identified priority watershed concerns for the RGH in the near-term future. To investigate these concerns, we used a modified version of the U.S. Geological Survey's Monthly Water Balance Model to produce modeled streamflow response to several single and overlapping disturbances over the years 2021-2050. Key findings from each scenario are presented below:

Model Scenario	Change Observed	Additional Context
Baseline (BUSINESS AS USUAL)	No change.	• This scenario did not include any land change or climate disturbances and was used as a point of comparison for the disturbance scenarios described below.
Hot-and-dry climate scenario	• Water yield *decreases* throughout each annual season, except during the rising limb of annual snowmelt, when water yield increases. • Decreases in annual water yield worsen with time, as climate gets progressively hotter and drier.	• As the climate provides less water and higher temperatures, the landscape experiences a higher demand for water. The result is decreased water yield in surface water bodies (i.e. streams and rivers).
Wildfire scenario	• Water yield *increases* throughout each annual season and produces the *greatest peak runoff* of all scenarios. • Post-fire runoff does return to the 'baseline' condition over time as vegetation reestablishes and the watershed recovers.	• While post-fire water yield impacts are substantial, wildfire impacts have been shown to be short-lived (Rust et al., 2019).
Overlapping wildfire & hot-and-dry climate scenarios	• These scenarios also predict *increases* in water yield throughout each annual season and produce the highest (and likely earliest) runoff of all scenarios during the rising limb of annual snowmelt. • Post-fire runoff shows gradual recovery (return to baseline condition) over time.	• When forest disturbances overlap, water yield changes are often difficult to detect (or are difficult to attribute to individual disturbances events) (Schneider et al, *in review*). • However, the use of models allows us to designate when/where disturbances occur, and to estimate their combined water yield impacts in a more-controlled way.
Overlapping forest-change and hot-and-dry scenario	• Does not alter water yield relative to the 'hot-and-dry' scenario.	• This scenario changed one forest type to another forest type and was likely not drastic enough to cause changes in water yield with this model. However, if a forest type were replaced with a non-forest type (e.g. grassland) water yield changes could be apparent.

Key takeaways from this work:

- Results from this work demonstrate that climate, and especially pre-disturbance ("antecedent") moisture conditions, have strong controls on post-fire surface runoff and recovery.
- Water managers should:
  - 1) Plan for a narrowing in the timing window of annual snow melt season (faster, earlier melt) regardless of disturbance type (e.g. climate or land cover).
  - 2) Consider antecedent moisture conditions when formulating their post-fire response plans, knowing that annual water yield and annual peak-runoff (RO_{pk}) will likely *temporarily* increase post-fire, but that dry antecedent conditions may result in earlier RO_{pk}, while wetter antecedent conditions may result in delayed RO_{pk}.
  - 3) For water supply predictions where source waters are in forested catchments (as is the case for much of Colorado's water supply), rely on hydrologic models that account for time-varying (dynamic) and quantitative vegetation change. Models lacking these elements likely will not adequately capture (or predict) water supply under dynamic forest health conditions.
  - 4) Encourage state and federal streamflow and snowpack monitoring efforts throughout the state of Colorado, and especially in Colorado's high forested watersheds.

Table of Contents

1. Background

Wildfires and bark beetle induced forest mortality are naturally occurring phenomena that have been part of North American ecosystems for millennia (Parker et al., 2006). While the relationship between bark beetle epidemics and wildfire is complex (Colorado State Forest Service, 2020) and often disagreed upon in the literature (Hicke et al., 2012; Fettig et al., 2021), both wildfires and insect induced forest mortality are undoubtedly exacerbated by drought (Kolb et al., 2016; Stephens et al., 2018). Wildfire is more likely when fuel is dry, and when trees are under water-stress, they often cannot adequately defend themselves against bark beetles (Fettig et al., 2021). As global temperatures increase, and severe drought becomes more commonplace (Cook et al., 2015), concern over the duration, frequency and severity of forest disturbances also mounts (Abatzoglou & Williams, 2016; Temperli et al., 2013; Westerling, 2006). Often, these forest disturbances occur in series (one disturbance creates optimal conditions for the next) or in parallel (co-occurring disturbances). In either case, multiple disturbances can have compounding effects on hydrologic processes. Disturbance signals are often variable at the stream outlet (Goeking & Tarboton, 2020), especially in the southern Rocky Mountains (Saxe et al., 2018), and are difficult to separate using observational before/after-control/impact (BACI) methods (Schneider et al, *in review*).

Traditional BACI methods rely on the assumption that the disturbance in question is the only (or most significant) difference between before-and-after disturbance periods, or between control-and-impacted sites. However, even when this assumption is true, co-occurring disturbances (as is often the case) are difficult to isolate at the stream outlet, especially when one disturbance mutes the hydrologic response of the other disturbance(s), such that the combined signal cannot be separated from natural streamflow variability. For example, drought is expected to decrease streamflow (Rood et al., 2008), and often occurs before, during or after wildfire, which is often expected to (at least temporarily) increase streamflow after vegetation is destroyed and evapotranspiration (ET) potential is lost (Goeking & Tarboton, 2020). Hydrologic models offer a viable tool for the problem of separating disturbance signals in observational (*in-situ*) datasets because they allow for true control over all variables contributing to streamflow variability (Penn et al., 2020). However, for hydrologic models to best capture forest disturbances, quantitative vegetation representation within the model is necessary (Goeking & Tarboton, 2020).

Since the early 2000s, Colorado's Rio Grande Headwaters (RGH) has experienced drought, widespread spruce beetle (*Dendroctonus rufipennis*) induced forest mortality (~2005 – 2011) and was extensively burned by the 2013 West Fork Complex (WFC) Fire. The RGH is mostly composed of alpine and subalpine forest ecoregions, which primarily host spruce-fir populations that thrive in the relatively cool and wet conditions found among subalpine forests (Colorado State Forest Service, 2014). Historically, wildfires have been more common in lower elevation forests that tend provide more optimal (warmer/drier) conditions for wildfire (Westerling, 2006). However, the 2013 WFC fire serves as a single example of a growing trend of wildfire occurrence in higher elevation forests (Alizadeh et al., 2021), and is likely attributable (at least in-part) to the decreasing snowpack trends and warming climate that have been observed in the RGH in recent decades (Chavarria & Gutzler, 2018; Sexstone et al., 2020). Snowpack that eventually becomes streamflow in the RGH is a critical natural resource to downstream water users in the San Luis Valley Irrigation District, several municipalities in Colorado and even downstream states that are entitled to receive annual flow volumes from

the Rio Grande (Rio Grande Compact, 1938). These recent forest disturbances have demonstrated that high elevation forest disturbances are of concern for the RGH stakeholders.

Certain disturbances are unlikely to occur again in the RGH for at least the next century; for example, another spruce beetle epidemic in the RGH is unlikely in the near-term future since the spruce population has already been extensively compromised and could take centuries to fully recover. However, the possibility of another large wildfire is feasible, as the majority of RGH forest remains unburned. Collaborative discussions among the Colorado School of Mines and RGH stakeholder groups[1] have identified climate change and wildfire (and especially the compounding hydrologic impacts of each) as priority concerns for the RGH. Although wildfire is arguably less-likely now than it was before the spruce beetle epidemic (dead spruce trees in their present grey phase have lower fuel loads (Hicke et al., 2012)), water managers are looking toward feasible worst-case scenarios to inform their future water planning efforts. Collaborative discussions have also identified climate-driven forest succession as a concern for the RGH because, as the warming and drying of higher elevations continues, distribution of vegetation may shift toward species that are better adapted to those conditions (Kelsey et al., 2018), especially following land cover disturbance (Stevens-Rumann & Morgan, 2019).

Water managers who rely on heavily forested drainages for their water supply, like those in the RGH, need planning tools capable of quantitatively representing vegetation changes to evaluate changes at the stream outlet. In this study, we modify the U.S. Geological Survey's (USGS) Monthly Water Balance Model (MWBM) to compute actual evapotranspiration (AET) based on empirically derived relationships between remotely sensed AET and a quantitative vegetation metric – leaf area index (LAI). The modified model version is referred to as MWBM-LAI. In addition to the development of MWBM-LAI, the goals of this study are to: 1) use this model to evaluate future forest disturbance scenarios that were identified as priority concerns by RGH stakeholders, and 2) to do so in a way that vets the hydrologic response to both singular and combined forest disturbances.

2. Modeling Methodology

2.1 Study Area & Model Domain

The Rio Grande Headwaters (RGH) serve as model domain for this study. We define the RGH as the portion of the Upper Rio Grande basin that drains into Del Norte, CO. Del Norte marks a particularly important point along the Rio Grande, because it is the first major decision-making point along the river, for determining quantities of water that must be sent to downstream users (Rio Grande Compact, 1938). The Rio Grande streamflow gage near Del Norte (USGS 08220000) is used as the design outlet for this study because 1) it provides a long period of record for streamflow (capturing flow from portions of the watershed that have previously experienced forest disturbance) and 2) flow there is mostly natural (it is located upstream of agricultural diversions in the San Luis Valley). However, several trans-basin ditches and reservoirs do exist within the RGH (upstream of Del Norte), but previous analyses have demonstrated that they do not significantly alter natural streamflow (Blythe & Schmidt, 2018; Chavarria & Gutzler, 2018).

---

[1] In this report, RGH stakeholder groups include: the Rio Grande Restoration Project, the San Luis Valley Water Conservancy District the Rio Grande Roundtable (of the Colorado Water Conservation Board), & the Rio Grande National Forest Service

The RGH is a heavily forested basin, consisting mostly of subalpine forests and includes some alpine, mid-elevation forests, grasslands and shrublands (US Environmental Protection Agency, 2012) – **Figure 1**. Since the early 2000s, the RGH has experienced substantial insect induced forest mortality and vegetation destruction from wildfire (Penn et al., 2020; Schneider et al., *in review*) – see Appendix **Figure A1**. Spruce beetle induced tree mortality impacted much of the forested portion of RGH from around 2000 – 2011; with much of the insect damage occurring between 2005 -2010 and tapering off around 2010-2011 (Schneider et al., *in review*; Sexstone et al., 2020). A few years later, the West Fork Complex Fire (initiated June 2013) burned large sections of the RGH, including both insect-impacted and undisturbed forest.
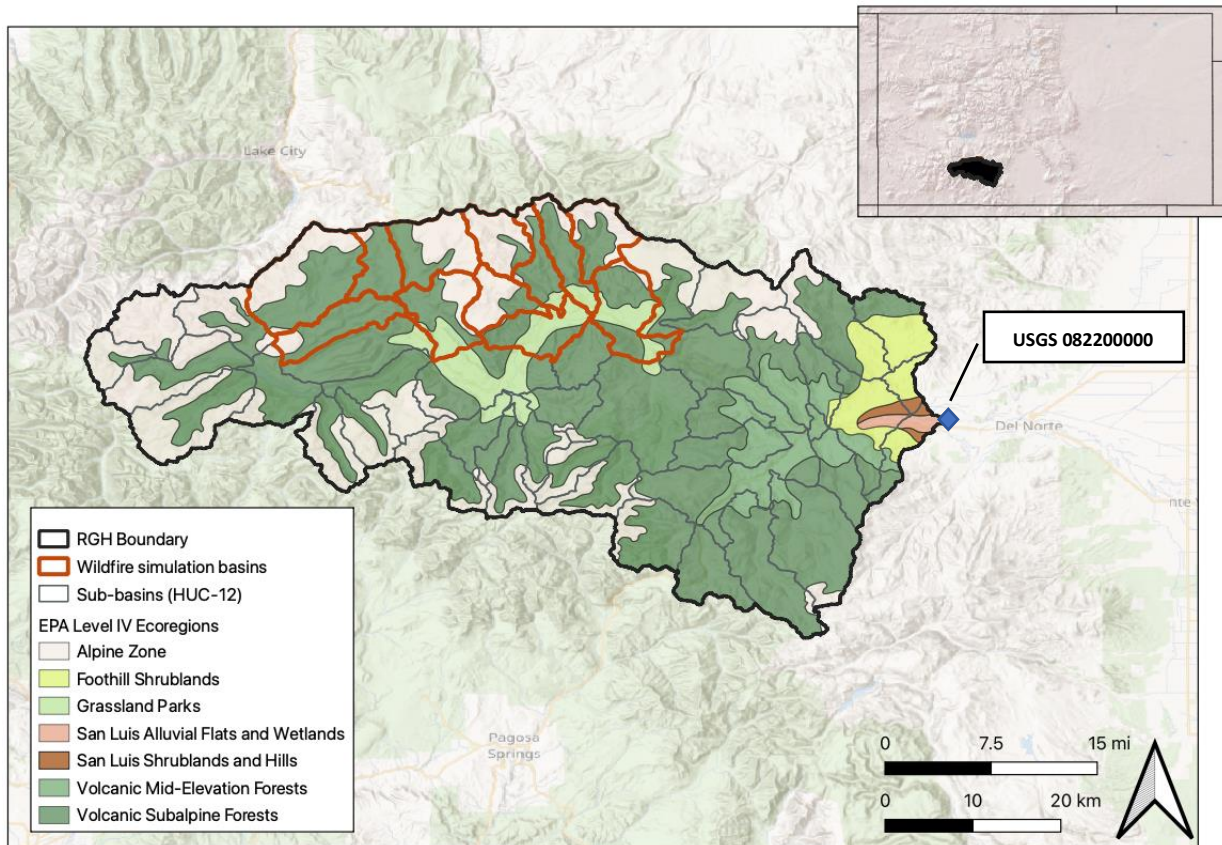
Figure 1 – Map of model domain with subbasins and EPA Level IV Ecoregions.
Inset map (top right), shows the RGH basin within state lines. The rectangle surrounding the RGH is the state of Colorado.

The RGH experiences a semi-arid climate, with most of the annual precipitation occurring as snow in colder months and most annual streamflow during warmer months when snow is melting. In recent decades, RGH precipitation has been trending downward and temperature has been trending upward (Sexstone et al., 2020; Chavarria & Gutzler, 2018). Several basins within the RGH have been observed as "water limited" (aridity index > 1), meaning that less water is available in those systems than what is demanded by the climate (Schneider et al., *in review*). The seasonal pulse in streamflow is highly variable in both timing and magnitude and depends on the amount of seasonal snowpack, as well as the rate of spring/summer snowmelt. Rising temperatures in the RGH contribute to an increasing ratio of

rain:snow in annual precipitation and may explain some of the streamflow variability (Chavarria & Gutzler, 2018).

Our model domain includes the RGH (delineated at the Del Norte gage), and is distributed into 51 sub-basins, where each sub-basin is a hydrologic unit code (HUC) 12 basin (**Figure 1**). Hydrologic unit code basins are maintained under the USGS Water Boundary Dataset and are commonly used in the USGS MWBM. The HUC-12 resolution was chosen because it provides basin delineations small enough to adequately characterize forest composition (level IV ecoregions and LAI) at the subbasin scale, without over-generalizing. Simulated streamflow from all sub-basins contributes to total simulated flow for the Rio Grande at Del Norte.

2.2 Data Sources

Climatic Data

Total monthly precipitation and average monthly temperature were sourced from the Parameter-elevation Regressions on Independent Slopes Model (PRISM) at 4-km resolution (PRISM, 2020). Daily actual evapotranspiration (AET) were taken from the Moderate Resolution Imaging Spectroradiometer (MODIS) MOD16A2 Version 6, at 500-m spatial and 8-day temporal resolutions (Running et al., 2017). Temperature, precipitation and AET rasters were aggregated to study basin polygons using a weighted extraction. Resulting AET extractions were cloud filtered (PRISM data did not require a cloud filter), removing observations where significant cloud cover was present with 75% or greater coverage (more stringent cloud filters greatly abbreviated the dataset). The resulting cloud-filtered dataset was gap-filled for single missing values by averaging nearest neighbors or for multiple consecutive missing values by assuming the previous 8-day observation.

Leaf Area Index

A 4-day Leaf Area Index (LAI) product was sourced from MODIS MCD15A3H Version 6, Level 4, at 500-m resolution. Leaf area index is a dimensionless canopy metric that represents the ratio of one-sided leaf area per unit ground area in broadleaf canopies and one half the total needle surface area per unit ground area in coniferous canopies (Myneni et al., 2015). A cloud correcting filter was applied to LAI, removing observations where significant cloud cover was present in study basins with 75% or greater coverage. Resulting 4-day cloud-filtered LAI observations were spatially aggregated to study basins using a weighted extraction, temporally aggregated to mean monthly LAI and were gap-filled following the method described above. MODIS-LAI data was the most temporally limiting dataset in this study as the available period of record only goes back to July 2002.

Runoff Data

Daily discharge [volume/time] data was sourced from the Rio Grande streamflow gage at Del Norte (USGS 08220000). These data were converted to surface runoff [depth/time] by normalizing discharge against the basin area and were further converted to total monthly runoff (RO) by summing daily RO values for each month.

Future Data Modifications

Modeled future disturbance scenarios required modification of some historic data. Specifically, future climate data was modified to a hot-and-dry scenario, following monthly

temperature offsets and precipitation adjustment factors from the Colorado Water Plan's 2019 Technical Update (Wlostowski, 2019) – **Table 1**. Details on the production of future climate data is described in greater detail in Section 2.4.

Table 1- Climate modifications for the hot-and-dry scenario ("7525 scenario")

Modifier	Jan	Feb	Mar	Apr	May	Jun	Jul	Aug	Sep	Oct	Nov	Dec	Annual Average
Precipitation change factor [-]	1.11	1.03	0.96	0.85	0.82	0.94	0.94	0.93	0.94	0.95	1.04	1.05	0.96
Temperature offsets [℃]	1.74	1.55	1.91	2.22	2.84	2.88	2.70	2.75	2.74	2.43	2.14	1.68	2.30

Future LAI data used in fire-scenarios also required modification to mimic conditions observed during the WFC fire of 2013. Changes in LAI were quantified for two well-studied sub-basins (Schneider et al., *in review*), including Trout Creek and Little-Squaw ("Little-S") Creek basins – which were burned at moderate-to-high burn severity at 21% and 20% area, respecitvely, during the 2013 WFC fire. These basins are mostly 'subalpine forest' and 'alpine' – and are well representative of other sub-basins burned during the WFC fire. The LAI changes observed in these basins after the WFC fire (**Table 2**), are used to modify LAI conditions for future fire scenarios. Here, we assume that post-fire changes in LAI are (in part) dependent on burn severity. So, by reproducing post-fire LAI changes, burn-severity is indirectly reproduced as well. However, from a hydrologic perspective, it is also important to note that burn severity does not only alter vegetation density, but it also changes soil surface properties, especially at higher burn severities (Ebel et al., 2016). The wildfire simulation is described in greater detail in Section 2.5 of this report.

Table 2- Changes in LAI after the WFC fire for Trout & Little-S Creek Basins
These changes are relative to a control period (July 2002 – Dec 2004), before insect damage was severe in these basins and before wildfire activity.

	Percent Change in LAI from Control Period [%]		
Time of Year	Fire Year (2013)	1-2 years post-fire (2014-2015)	3-4 years post-fire (2016-2017)
Warm months [June - Sept]	-20.6	-6.0	0.7
Cold months [Oct - May]	-49.1	-47.1	-44.4

2.3 Model description

The U.S. Geological Survey's (USGS) Monthly Water Balance Model (MWBM) is a water budget accounting tool that has been used to evaluate water budgets under many climatic conditions (McCabe & Wolock, 2008; Hay & McCabe, 2010; Bock et al., 2016) including as a component of the USGS National Hydrologic Model (NHM) where its monthly simulations are used to constrain a daily hydrologic model (Regan et al., 2019). The original MWBM computes surface water budget components at a monthly time step and is driven by mean monthly temperature, total monthly precipitation, and latitude for the computation of day length; used to compute potential evapotranspiration (PET) following the Hamon equation (Hamon, 1961).

This description focuses on the MWBM's computation of evapotranspiration (ET), however, for an in-depth description of the MWBM accounting procedure, see McCabe & Markstrom, 2007. Under relatively dry conditions, actual evapotranspiration (AET) is computed as a function of snow melt, precipitation (not routed to direct surface RO) and soil moisture conditions. Under relatively wet conditions, AET is equal to PET. Thus, in either case (relatively wet or dry conditions), the original MWBM does not account for vegetation in its computation of ET – ultimately limiting its usefulness as a tool to evaluate hydrologic implications after land cover disturbance.

For this study, we develop a modified version of the original MWBM, called *"MWBM-LAI"* which relies on LAI for the computation of AET. To achieve this, the AET computation module in the original MWBM (described above) was simply replaced with a new AET computation module based on empirically derived relationships between AET and LAI in the RGH. The inclusion of this LAI-based AET computation does require monthly LAI as an additional model forcing dataset.

Derivation of empirical relationships between observed AET and LAI is described as follows. First, each HUC-12 sub-basin in the RGH was designated as its "dominant" ecoregion type. For example, if the majority of a sub-basin's land cover area was 'subalpine forest', that sub-basin was designated as "subalpine forest dominant". Next, for subbasins of each dominant ecoregion, monthly LAI was plotted against monthly ET, and linear regressions were performed to model ET as a function of ET. Separate regressions were performed for warm months (Jun – Sept) and cold months (Oct -May). Linear regressions enforced a zero y-intercept, to account for our assumption that ET is primarily controlled by vegetation, especially during warm months. While five dominant ecoregions are present throughout RGH sub-basins, four sets of ET-LAI empirical relationships were developed, because 'alpine' and 'subalpine forest' ecoregions exhibited extremely similar ET-LAI empirical relationships. Empirically derived coefficients for dominant ecoregions are summarized in **Table 3**.

Table 3- Empirically Derived Coefficients for Linear Models of ET -vs- LAI
Following y = mx + b, where (b = 0) such that: ET = m(LAI).

		Alpine/subalpine forests	Mid-elevation forests	Grassland parks	Foothill shrubland
Warm months [Jun – Sept]	Intercept	0	0	0	0
	Slope	44.76	35.73	40.68	35.58
	R^2	0.96	0.97	0.96	0.96
Cold Months [Oct – May]	Intercept	0	0	0	0
	Slope	75.01	51.94	74.14	65.99
	R^2	0.65	0.83	0.83	0.71
Based on:		*10 'alpine' and 'subalpine forest' dominant HUCs mostly free of insect mortality and burn between July 2002-Dec 2006.*	*'Mid-elevation forest' dominant HUCs between July 2002 - Oct 2020.*	*'Grassland park' dominant HUCs between July 2002 - Oct 2020.*	*'Foothill shrubland' dominant HUCs between July 2002 - Oct 2020.*

The only other modification to the original-MWBM was the addition of seasonal precipitation adjustment factors or "*pfactors*". Following the methodology described by Hay & McCabe (2010), seasonal *pfactors* were added to the MWBM-LAI and were calibrated along with the other six standard calibration parameters. Seasonal *pfactors* adjust precipitation

forcing data by some factor; either increasing precipitation (if *pfactor* >1) or decreasing precipitation (if *pfactor* < 1). Based on comparisons between PRISM-based precipitation and *in-situ* precipitation observations from SNOTEL stations within the RGH, PRISM-based precipitation tends to underestimate winter precipitation and overestimate summer precipitation, especially during monsoon season. Thus, we felt the addition of seasonal *pfactors* to existing calibration parameters was necessary. Calibrated *pfactor* values are summarized in the Appendix (**Table A1**).

2.4 Model Calibration & Validation

To meet the needs of various scenarios, the MWBM-LAI is calibrated to two different time periods; once before the 2013 WFC fire to establish a 'baseline' parameterization and once after the WFC fire to establish a 'fire parameterization'. Due to changes in surface conditions after moderate-to-severe burn, a unique fire-parameterization was necessary. For the baseline parameterization, MWBM-LAI was calibrated against observed streamflow at the Del Norte gage for water years 2007-09 (October 2006 – September 2009), and validated for water years 2010-12 (October 2009-September 2012) (**Table A1**). To allow adequate time for model spin-up (ideally 4-5+ years), and to stay within the constraints of the MODIS-LAI period of record (begins July 2002), the calibration window could not start earlier than WY 2007. The MWBM-LAI was also calibrated after the WFC fire over the period of June 2013 – December 2017 – to capture both the fire year (2013) and 4 post-fire years (2014-2017). This window is referred to as the "post-fire evaluation period" since the model was calibrated to these conditions but could not be validated against another fire period. For scenarios involving fire, a dynamic combination of baseline parameters and fire-specific parameters were employed. We define a 'dynamic parameterization' as one that changes throughout the simulation period to represent changing physical conditions within the study domain. This differs from a traditional parameterization which employs stationary parameter values throughout the simulation period.

During each calibration period, 20,000 parameter combinations were tested. Parameter sets were generated following a Latin Hypercube Sampling (LHS) procedure, which breaks the parameter space into strata, and uniformly samples each strata, resulting in less-biased sampling with a smaller number of samples (relative to non-uniform sampling methods like Monte Carlo). Parameter set performance was determined by comparing modeled RO against observed RO using both Nash Sutcliffe Efficiency and percent-bias as objective functions. NSE is the magnitude of model residual variance to the variance of observed data (Nash & Sutcliffe, 1970).

- **Nash Sutcliffe Efficiency (NSE)** ranges from negative infinity to 1; where NSE = 1 suggests a perfect relationship between modelled and observed data, NSE = 0 indicates that the model is as arcuate as the mean of observed data, and NSE < 0 reveals that the mean of observed data is a better predictor than the model.
- **Percent bias (pbias)** gives the average tendency of modeled values to be greater than or less than observed values. Zero pbias is optimal, while positive and negative pbias indicate model overestimation and underestimation, respectively.

Percent-bias and NSE were computed using the 'hydroGOF' library package in the statistical software R (Zambrano-Bigiarini, 2020). A '50/50 score', equally weighting scores of

NSE and pbias was used as the primary comparative metric (**Equation 1**), where a score of '100' is a perfect score.

$$50/50 score = \ 0.5(NSE * 100) + (0.5|pbias|(-1) + 100) \qquad \textbf{Equation 1}$$

The top four scoring values from the 20,000 LHS parameter sets tested during calibration were also scored during the validation period. Parameters that performed best in both calibration and validation were selected for the baseline parameterization. Since validation was not possible for the fire-parameterization, the top scoring parameter set was selected from calibration. Parameter values and comparative metrics are summarized in **Table A1**.

2.5 Future Streamflow Scenarios

To approximate future flow conditions under various natural disturbances, MWBM-LAI was used to model four disturbance scenarios in addition to a baseline scenario (**Table 4**). These scenarios model future surface RO over the period: 2021-2050 and are described below. The year 2050 was selected as the endpoint for these simulations for two reasons; 1) it is close enough to the present date for RGH water managers to realize near-term potential water availability outcomes, and 2) this end date is congruent with climate projections in the 2019 Colorado Water Plan Technical Update (Wlostowski, 2019) that water managers already look to for guidance. Note: all LAI and climate-forcing data sets used for future scenarios also include a 5-year spin-up window, representing years 2016-2020. The 5-year spin-up window is made up of the first simulation year (2021), repeated five times. The purpose of this spin-up window is to allow time for model storage ("buckets") to fill, prior to the simulation period of interest.

- **Baseline scenario**- This scenario is used is used as the reference condition for all disturbance scenarios. Baseline parameterization is used here. No adjustments are made to baseline LAI-forcing data, or baseline climate-forcing data. Baseline LAI data is derived from monthly averages of LAI over a period of minimal disturbance in the RGH; July 2002 – December 2007. Monthly average LAI values are repeated 30 times to produce 30 years of future LAI data. Baseline climate data is produced by repeating PRISM-based monthly mean temperature and monthly total precipitation for 10 recent historic years (2011-2020) in triplicate to produce 30 years of future climate data.
- **"Climate only" scenario** – No modifications are made to LAI-forcing data, however baseline climate-forcing data is altered toward hot-and-dry conditions by linearly scaling precipitation down (to max-dryness in 2050) and linearly scaling temperature up (to max-temperature) in 2050. See **Table 1** for the scaling factors used to adjust climate. Baseline parameterization is used.
- **"Fire only" scenario**- No modifications are made to baseline climate data, however some modifications are made to LAI-forcing data, and the fire-scenario parameterization is employed during the fire period (2041-2045). Here, LAI-forcing data are reduced at the initiation of fire (June 2041) and four post-fire years (through 2045). LAI reductions are based on observations of reduced LAI after the 2013 WFC fire (**Table 2**) which also began during the month of June and burned 'alpine' and 'subalpine' dominant sub-basins within the RGH. To mimic these conditions for a future fire scenario, historical observations of LAI reductions (after the WFC fire) are applied to 12 previously un-burned 'alpine' and 'subalpine forest' dominant sub-basins (**Figure 1** – see sub-basins

outlined in orange). This approach was taken because the WFC fire burned at least 20%-area of 12-HUC basins in the 'alpine' and 'subalpine-forest' zones, at moderate-to-severe burn severity. In this way, the fire scenario replicates the extent, burn severity (through reductions in LAI), and forest type that were observed during the 2013 WFC fire. However, this scenario simulates these conditions in a portion of the RGH that has not recently experienced wildfire and still has fuel available to burn.

- **"Fire + Climate" scenarios** – All modifications to both "climate only" and "fire only" scenarios are applied here – including modified LAI-forcing data, hot-and-dry climate-forcing data, and the fire-scenario parameterization during the fire period. This scenario is modeled twice: once with fire initiating in June 2013 and again in June 2041. The occurrence of fire seems more likely during the 2041-2050 decade, because that decade is the hottest and driest decade during the simulation period and because it is temporally further removed from the 2013 WFC. However, a fire was also simulated during the 2031-2040 decade, to observe a longer window of post-fire hydrologic recovery.
- **"Climate + forest change" scenario** – Hot-and-dry climate-forcing data are used here. Baseline parametrization is employed. To simulate this change in forest cover, one third of sub-basins (17 HUC-basins) in the lowest forested portion of the RGH are converted from 'subalpine forest' dominant (mostly spruce-fir trees that prefer cool/wet environments) to 'mid-elevation forest' dominant (more pine and other tree species trees that can thrive in warmer condition). In converting these forest types, AET is computed in converted basins according to the empirical relationship of ET-LAI for a 'mid-elevation forest' type. These changes are applied to the entire simulation period.

Table 4- Disturbance Scenarios Summary

Scenario	Parameterization	LAI adjustment	Climate
Baseline	Baseline parameters	Baseline LAI	Baseline climate
Climate only (hot/dry)	Baseline parameters	Baseline LAI	Hot/dry climate
Fire only	Dynamic parameter combination- using calibrated fire parameters during fire window: 2041-2045; otherwise, baseline parameters.	LAI adjusted during fire window: 2041-2045.	Baseline climate
Climate (hot/dry) + fire	Dynamic parameter combination- using calibrated fire parameters during fire window: 2041-2045; otherwise, baseline parameters.	LAI adjusted during fire windows: (a) 2031-2035 and (b) 2041-2045.	Hot/dry climate
Climate (hot/dry) + forest change	Baseline parameters	LAI is indirectly adjusted for entire simulation window by converting 1/3 of subbasins from 'subalpine forest' to 'mid elevation forest'.	Hot/dry climate

3. Modeling Results

The following results describe modeled RO scenarios for each decade within the future simulation period (2021-2052). The 2021-2031, 2031-2040 and 2041-2050 decades are referred to as the "first decade", "middle decade" and "last decade", respectively.

3.1 Decadal Results

The baseline scenario is used as the reference condition for all modelled scenarios. **Table 5** shows decadal deviations (percent-change) in scenario RO from baseline RO for: annual total, melt season (April – June), monsoon season (July – September), and a low flow period (October – December). All scenarios involving climate change show progressive decreases in runoff over time, while all scenarios involving fire show notable increases in RO for the decades during and after fire. The "Forest Change + Climate" scenario matches the "Climate Only" scenario, likely because changing one forest type to another forest type ("subalpine forest" to "mid-elevation forest") is not a major-enough change in vegetation to produce a shift in RO. The greatest increase to RO occurs in the "Fire 2041 Only" scenario, the greatest decrease to RO occurs during the "Climate Only" scenario, while scenarios involving both climate change and fire produce RO somewhere between the two extremes. Generally, the greatest deviations from the baseline condition are observed in the last modelled decade, as this is when modeled climate change is the most severe during the simulation period and because two of the three fire-scenarios initiate burn during the last decade. The only exception to this is with the "Fire 2031 + Climate" scenario, where the greatest deviations from baseline are observed during the middle decade (when fire was simulated). In the last decade after the simulated 2031 fire, RO levels do shift back toward the baseline condition (especially during the low flow period), however flows stay elevated into the last decade.

From a seasonal angle, the greatest deviations in fire scenarios occur during the low flow period and melt season. However, the greatest shift in the "Climate Only" scenario is observed during monsoon season. Computing the percent-change in small numbers can result in elevated percentages. Thus, high percent-changes observed during monsoon season and the low flow period do not reflect the highest *absolute* changes in RO. Absolute changes in decadal RO for each scenario are presented in the Appendix (**Table A1**).

**Table 5 – Decadal Results Summarized by Flow Seasons**

*Absolute values of RO per season and scenario are included in the Appendix as **Table A2**.*

		Runoff Percent-change from Baseline [%]						Color Key:
	Decade	Climate Only	Forest Change + Climate	Fire 2041 Only	Fire 2041 + Climate	Fire 2031 + Climate		
Average Annual Runoff Total	2021-30	-2.4	-2.4	0.0	-2.4	-2.4		< (-30) %
	2031-40	-8.7	-8.5	0.0	-8.5	27.8		(-30) - (-20) %
	2041-50	-14.4	-14.2	32.0	23.9	20.4		(-20) - (-10) %
Average Melt Season Runoff Total [Apr - Jun]	2021-30	0.7	0.7	0.0	0.7	0.7		(-10) - 0 %
	2031-40	-3.6	-3.6	0.0	-3.6	24.4		0%
	2041-50	-10.0	-10.0	17.1	19.9	19.3		0 - 10 %
Average Monsoon Season Runoff Total [Jul - Sept]	2021-30	-10.8	-10.8	0.0	-10.8	-10.8		10 - 20%
	2031-40	-26.2	-26.2	0.0	-26.2	48.8		20 - 30%
	2041-50	-38.9	-38.9	81.2	16.2	14.2		> 30 %
Average Low-Flow Runoff Total [Oct-Dec]	2021-30	-0.2	-0.2	0.0	-0.2	-0.2		
	2031-40	1.1	1.1	0.0	1.1	46.4		
	2041-50	6.0	6.0	85.8	21.0	3.7		

3.2 Final Decade (2041-2050) Results

The greatest deviations in simulated RO are observed during the last decade of the simulation period. This section focuses on changes in the magnitude and timing of simulated RO for the last decade. Note: the "Forest Change + Climate" scenario is not included here for the sake of simplicity, and ultimately because it matches results from the "Climate Only" scenario. Only the two fire scenarios that simulate fire in the fire in the last decade are included here, for comparability.

Simulated RO for the last decade was broken down into magnitude quartiles; low (Q0-25%), low-moderate (Q25-50%), high-moderate (Q50-75%) and high (Q75-100%) and are shown in **Figure 2**. Except for low-moderate RO (Q25-50%), RO for "Climate Only" is always lower than baseline. For all flow magnitudes, RO in fire scenarios is always higher than baseline. Per quartile, the greatest absolute variability in RO occurs in the high RO (Q75-100%) quartile and the lowest absolute variability in RO occurs in the low RO (Q0-25%) quartile. However, the most notable RO deviations from baseline occur in the low RO quartile, where RO for "Climate Only" is slightly lower than baseline, but both fire scenarios are nearly an order of magnitude higher than baseline.
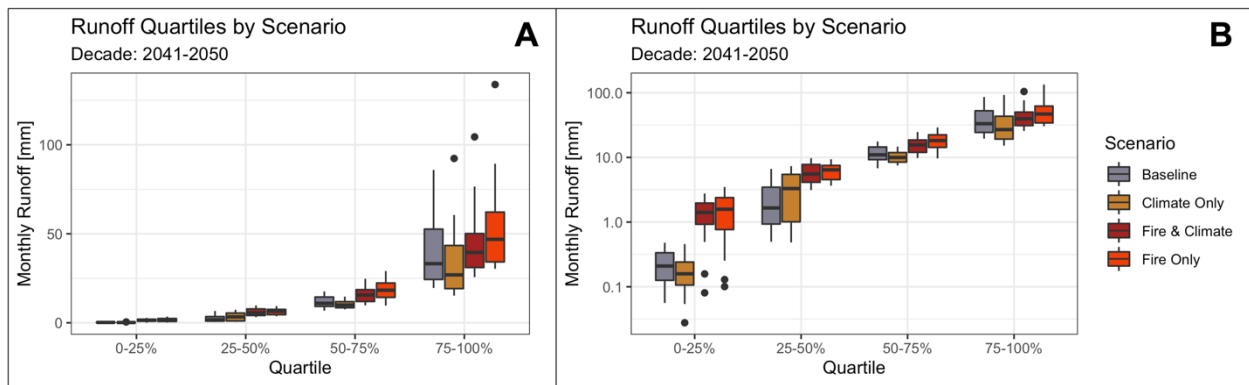
Figure 2- Simulated runoff quartiles for the last simulation decade.

A) axes are untransformed. B) y-axis is log-transformed for ease of viewing low RO values.
Note: Changes in flow magnitude for the last decade are also shown as flow duration curves (FDCs) in the Appendix (Figure A2).

To capture how runoff magnitude in the last simulation decade changes throughout an annual cycle, monthly runoff averages and standard deviations are shown in **Figure 3A** and **Figure 3B**, respectively. Simulated runoff in **Figure 3** generally agrees with previous results. However, with this presentation, a few several notable timing trends are now evident. First, "Fire Only" RO peaks a month later (June) than RO from all other scenarios (which peak in May) and experiences the most variable RO (shown by the shaded region in **Figure 3B**) as well as the highest peak RO (RO_{pk}). Relative to baseline, all scenarios experience a more rapid rise in RO during the annual rising limb (March to April). RO for all scenarios exceeds baseline on the rising limb, however during the annual recession (~June-August), "Climate Only" RO is the only scenario lower than baseline.
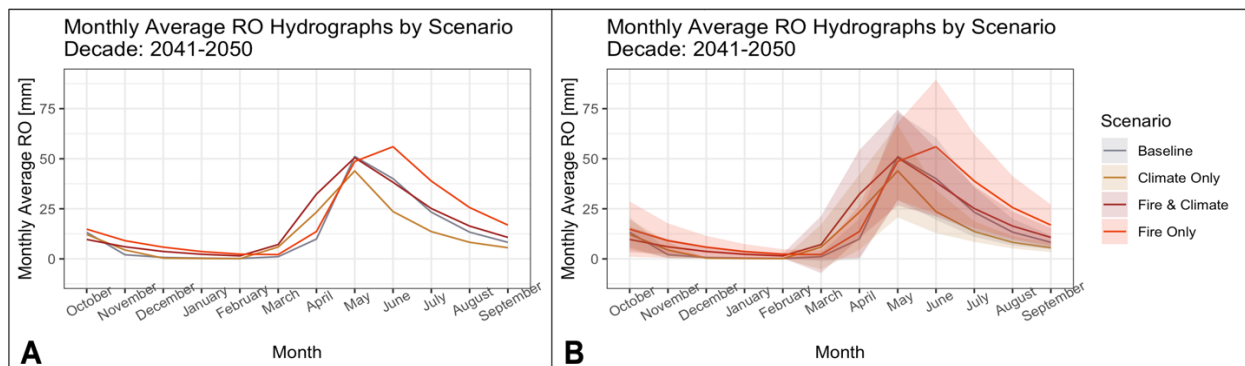
Figure 3- Mean monthly RO (A) and standard deviation (B) for each scenario during the last simulation decade.

In both A and B plots, the bold lines show mean monthly RO during the last simulation decade. The shaded ribbons in plot-B represent one standard deviation above and below the mean, to illustrate the variability of RO during the last simulation decade.

4. Discussion of Results

One of the greatest advantages offered by hydrologic models is their ability to control all variables that influence a hydrologic flux, thereby allowing for 1) the creation of truly controlled reference conditions and 2) scaffolded introduction of disturbance scenarios. In this study, we

adapted a hydrologic model to capture both the individual and combined effects of various land cover disturbances at the stream outlet; a task that is challenging using observational datasets alone. These efforts were made possible by the inclusion of quantitative vegetation representation (LAI) in the MWBM's water budget accounting procedure, and by developing dynamic parameterizations for the model.

However, like all modeling approaches, the methodology developed in this study has limitations. Perhaps most notably, is that the inclusion of LAI in the model primarily controls AET (and indirectly controls soil moisture and surface runoff), however, LAI does not influence modeled snow water equivalent (SWE). Changes in forest canopy have been shown to alter snow accumulation and removal (sublimation/melt) rates (Gleason et al., 2019). Thus, vegetative controls on snowpack are an important part of the hydrologic "story" that are not included in this modeling effort. This may justify (in part) the lack of RO change observed between the "Climate Only" and "Forest Change + Climate" scenarios (**Table 5**). For example, if LAI within the model had any control over SWE computation, a change in forest structure ('subalpine forest' to 'mid-elevation forest') might have been more pronounced at the stream outlet. It is also plausible that changing one evergreen forest type to another evergreen forest type is truly not drastic enough (from either SWE or ET angles) to cause notable change in RO. The empirical LAI-ET relationships developed for alpine/subalpine and mid-elevation were based on observations of LAI and ET basins that were *mostly* free of insect induced forest mortality (it was not possible to choose basins entirely free of insect mortality). The minor presence of spruce beetles in those basins (or occurrence of drought) could have dampened the RO signal from the forest change scenario. However, changing a forest type to a more-different land cover (e.g. grassland or shrubland, as is sometimes observed post-fire (Stevens-Rumann & Morgan, 2019)), would produce greater changes in RO. The question of forest succession on streamflow response, and especially how-to best represent forest succession in hydrologic modeling tools, warrants additional study.

Relative to baseline, the greatest increases in flow magnitude for all RO quartiles and for RO_{pk} are observed in the "Fire Only" scenario. Others have also predicted substantial increases in modeled post-fire streamflow in the RGH, using historic hydroclimatic data (Penn et al., 2020). The greatest variability in RO is also observed in the "Fire-Only" scenario, which agrees with previous observations of high variability in post-fire runoff in the Southern Rocky Mountain region (Saxe et al., 2018). Since a baseline climate is used in the "Fire Only" scenario (which is the "wetter" climate scenario of the two), more water is available to runoff. During the fire-only simulation, land cover conditions are changed to reflect decreased vegetation cover (and consequently decreased ET) and surface conditions are adjusted (via fire-specific parameterization) to reflect the post-fire environment. The combination of 1) reduced ET, 2) changes in post-fire surface conditions and 3) greater water availability create optimal conditions for increased RO throughout the annual water cycle. Not only is RO_{pk} higher for the "Fire Only" scenario, but it is also a month later than all other scenarios (RO_{pk} in June rather than May). This is driven in-part by the chosen month for fire simulation (June), which caused a large spike in RO during the month of June and skews decadal timing results toward delayed RO_{pk}. Still, the snowmelt RO recession also shows elevated RO for both fire scenarios, which reflects decreased ET during those warm summer months (making more water available for RO). Reductions in ET (as well as altered surface conditions) also explain elevated RO during lower-flow periods for both fire scenarios. Specifically, when less moisture is drawn out of soil

stores during warm months, a higher subsurface moisture content is available to support RO during low-flow periods.

The opposite is true for the "Climate Only" scenario, where vegetation and surface conditions mimic baseline, but climate is hotter and drier. Overall, the greatest decreases in flow magnitude occur in the "Climate Only" scenario, with the exceptions of low-moderate RO (Q25-50%) and RO_{pk}. With less water available to runoff in the "Climate Only" scenario, it is counter-intuitive that RO could exceed baseline RO any time of year. However, increases in melt season temperature drive increases in RO during the "rising limb" of the annual melt season, as well as RO_{pk}. These increases are balanced by a more rapid decline in RO during the snowmelt recession and during low-flow periods.

Not surprisingly, runoff during the "Climate + Fire" scenario generally falls somewhere between the "Climate Only" and "Fire Only" scenarios. However, a few times throughout the year this is not the case. During the rising-limb of annual snowmelt, RO during the "Fire + Climate" scenario increases more rapidly than all other scenarios and has the highest RO_{pk} during the month of May. The combination of post-fire changes in land surface conditions, as well as increased temperature, drive this fast and high RO trend during melt season. A caveat of using a monthly resolution water budget model is that changes in RO timing that are less than one full month will not be explicitly detected by the model. However, since "Fire + Climate" RO shows the fastest and highest trend, it is likely that RO_{pk} does occur earlier (on the order of days to weeks) than baseline RO. Given that the only difference between the "Fire Only" and "Fire + Climate" scenarios is climate, yet the timing and magnitude of their respective RO_{pk}'s are quite different; this strongly points toward antecedent conditions having robust controls on the outcome of both the timing and magnitude of post-fire streamflow and recovery (McMillan et al., 2018; Moeser & Douglas-Mankin, 2017) . Drier antecedent conditions under the hot-and-dry climate scenario result in less stored water (e.g. soil moisture and snowpack) to supplement RO.

5. Conclusions & Recommendations

In this work, we incorporate quantitative vegetation representation into a monthly resolution water balance model and utilize a dynamic parameterization to model both singular and overlapping watershed disturbances over the future period 2021-2050. A hot and dry climate simulation alone decreases water yield throughout each annual season, except during the rising limb of annual snowmelt, when warm temperatures drive more rapid RO. A fire simulation alone (similar in magnitude to the 2013 WFC fire) increases water yield throughout each annual season and produces the greatest and most-delayed RO_{pk}. A combined fire and hot-and-dry climate simulation point to earlier and higher annual RO_{pk} under these conditions. A combined forest-change and hot-and-dry simulation does not change RO relative to the climate-only simulation. These results demonstrate that climate, and especially antecedent hydrologic conditions, have strong controls on post-fire surface runoff and recovery. So, while future climate outcomes and the onset of wildfire remains uncertain, water managers should: 1) plan for a narrowing in the timing window of annual melt season (faster, earlier melt) regardless of disturbance type (e.g. climate or land cover) and 2) consider pre-fire watershed conditions when formulating their post-fire response plans, knowing that annual water yield and RO_{pk} will likely *temporarily* increase post-fire, but that dry antecedent conditions may result in earlier RO_{pk}, while wetter antecedent conditions may result in delayed RO_{pk}.

In addition to changes in the timing and magnitude of annual water yields, water managers should also prepare for temporarily impacted water quality after wildfire. While water quality was not explored in this study, others have observed compromised water quality after the 2013 WFC fire in the RGH (Rust et al., 2019). Specifically, Rust and others observed increases in sediment loading from steep severely burned hillslopes in tributaries to the Rio Grande. Consequently, post-fire turbidity was elevated for at least three years after the WFC fire and was ultimately responsible for acute fish kills immediately following the fire. Water managers should be weary of post-fire sedimentation after large rain events, and especially during monsoon season in the RGH, as post-fire precipitation events are responsible for dislodging sediments. Topographic (e.g. slope steepness) and hydro-climatic (e.g. precipitation, streamflow) variables have controls on the degree of post-fire stream sedimentation (Silins et al., 2009).

Beyond the RGH, much of Colorado's land surface is covered by semi-arid high elevation alpine and subalpine forests. These regions receive a vast majority of Colorado's annual water supply in the form of snowpack. As land cover and climate disturbances continue to disrupt Colorado's mountains, understanding the hydrologic impacts of these disturbances and developing predictive tools for water supply planning is more urgent than ever – for Colorado, and all downstream states who rely on Rocky Mountain snowpack. This study is a good first step toward understanding and modeling hydrologic change after disruptions to Colorado's high forests, however, more work is critically needed to capture hydrologic disruptions over larger areas.

The empirical relationships and modeling framework developed in this study have strong potential to inform future modeling efforts in burned and/or semi-arid high elevation catchments – whether with the Monthly Water Balance Model or other hydrologic models. The model framework described here is likely transferrable to other models that already have either 1) quantitative vegetation representation built-in or 2) the ability to modify ET modules (and/or snow and soil moisture modules) so that the mathematical representation of those processes can account for quantitative vegetation change. A modeling application such as the one presented here is feasible for a larger portion of the Rio Grande River basin, or even for the state of Colorado and hydrologically connected areas. However, this study, along with recent forest hydrology literature (Goeking & Tarboton, 2020) illustrates the importance of including *quantitative* vegetation representation in hydrologic models that are used to predict water supply changes associated with forest disturbance. Given that much of Colorado's water supply originates in high mountain forested catchments that are constantly experiencing disturbance (drought, insect/disease induced forest mortality, wildfire, forest removal, development, etc.), large scale water supply modeling efforts *must account for vegetation change* to adequately capture and predict Colorado's water supply under dynamic forest health conditions. For water supply modeling efforts in Colorado's forested catchments, we do not recommend the use of hydrologic models lacking these elements. When a hydrologic model includes time varying vegetation information, not only will this allow the model to capture an initial disturbance (e.g. vegetation removal from wildfire) but it will also enable the model to capture the dynamic post-disturbance recovery process (e.g. regrowth after burn). Cross-discipline coordination between hydrologists and state and federal forest managers will be essential for future modeling efforts.

Other challenges and considerations for expanding this work to a larger domain, include: quantifying the many diversions and agricultural water uses in Colorado (and representing those anthropogenic water applications within a model), and obtaining hydrologic

datasets (e.g. streamflow, snowpack, etc.) with adequate spatial and temporal coverage of Colorado's forested catchments. The Monthly Water Balance Model is capable of accounting for anthropogenic water use, however, other models that are structured to capture anthropogenic water-use and water-quality implications may be better outfitted for the task and should be considered if a larger domain modeling efforts are undertaken. Additionally, continued installation and operation of streamflow gages (such as those maintained by the Colorado Division of Water Resources or the USGS) and Snow Telemetry (SNOTEL) sites across Colorado's forested basins will greatly support (and improve) predictive water supply modeling efforts throughout the state.

6. Bibliography

Abatzoglou, J. T., & Williams, A. P. (2016). Impact of anthropogenic climate change on wildfire across western US forests. *Proceedings of the National Academy of Sciences of the United States of America*, *113*(42), 11770–11775. https://doi.org/10.1073/pnas.1607171113

Alizadeh, M. R., Abatzoglou, J. T., Luce, C. H., Adamowski, J. F., Farid, A., & Sadegh, M. (2021). Warming enabled upslope advance in western US forest fires. *Proceedings of the National Academy of Sciences of the United States of America*, *118*(22). https://doi.org/10.1073/pnas.2009717118

Blythe, T. L., & Schmidt, J. C. (2018). Estimating the Natural Flow Regime of Rivers With Long-Standing Development: The Northern Branch of the Rio Grande. *Water Resources Research*, *54*(2), 1212–1236. https://doi.org/10.1002/2017WR021919

Bock, A. R., Hay, L. E., McCabe, G. J., Markstrom, S. L., & Atkinson, R. D. (2016). Parameter regionalization of a monthly water balance model for the conterminous United States. *Hydrology and Earth System Sciences*, *20*(7), 2861–2876. https://doi.org/10.5194/hess-20-2861-2016

Chavarria, S. B., & Gutzler, D. S. (2018). Observed Changes in Climate and Streamflow in the Upper Rio Grande Basin. *Journal of the American Water Resources Association*, *54*(3), 644–659. https://doi.org/10.1111/1752-1688.12640

Colorado State Forest Service. (2014). *Spruce Beetle- Quick Guide Series FM 2014-1*. https://csfs.colostate.edu/media/sites/22/2014/02/Spruce-Beetle-QuickGuide-FM2014-1.pdf

Colorado State Forest Service. (2020). *2020 Report on the Health of Colorado's Forests*. https://csfs.colostate.edu/media/sites/22/2021/02/CSFS_2020_Forest_Health_Report_WEB.pdf

Cook, B. I., Ault, T. R., & Smerdon, J. E. (2015). Unprecedented 21st century drought risk in the American Southwest and Central Plains. *Science Advances*, *1*(1), 1–8. https://doi.org/10.1126/sciadv.1400082

Ebel, B. A., Rengers, F. K., & Tucker, G. E. (2016). Observed and simulated hydrologic response for a first-order catchment during extreme rainfall 3 years after wildfire disturbance. *Water Resources Research*, *52*, 9367–9389. https://doi.org/10.1111/j.1752-1688.1969.tb04897.x

Fettig, C. J., Hood, S. M., Runyon, J. B., & Stalling, C. M. (2021). Bark Beetle and Fire Interactions in Western Coniferous Forests : Research Findings. *Fire Management Today*, *79*(1), 14–23. https://www.fs.fed.us/psw/publications/fettig/psw_2021_fettig006.pdf

Gleason, K. E., McConnell, J. R., Arienzo, M. M., Chellman, N., & Calvin, W. M. (2019). Four-fold increase in solar forcing on snow in western U.S. burned forests since 1999. *Nature Communications*, *10*(1), 1–8. https://doi.org/10.1038/s41467-019-09935-y

Goeking, S. A., & Tarboton, D. G. (2020). Forests and water yield: A synthesis of disturbance effects on streamflow and snowpack in Western coniferous forests. *Journal of Forestry*, *118*(2), 172–192. https://doi.org/10.1093/jofore/fvz069

Hamon, W. R. (1961). Estimating potential evapotranspiration. *Journal of the Hydraulics Division, Proceedings of the American Society of Civil Engineers*, *87*, 107–120.

Hay, L. E., & McCabe, G. J. (2010). Hydrologic effects of climate change in the Yukon River Basin. *Climatic Change*, *100*(3), 509–523. https://doi.org/10.1007/s10584-010-9805-x

Hicke, J. A., Johnson, M. C., Hayes, J. L., & Preisler, H. K. (2012). Effects of bark beetle-caused tree mortality on wildfire. *Forest Ecology and Management*, *271*, 81–90. https://doi.org/10.1016/j.foreco.2012.02.005

Rio Grande Compact, (1938).

Kelsey, K. C., Redmond, M. D., Barger, N. N., & Neff, J. C. (2018). Species, Climate and Landscape Physiography Drive Variable Growth Trends in Subalpine Forests. *Ecosystems*, *21*(1), 125–140. https://doi.org/10.1007/s10021-017-0139-7

Kolb, T. E., Fettig, C. J., Ayres, M. P., Bentz, B. J., Hicke, J. A., Mathiasen, R., Stewart, J. E., & Weed, A. S. (2016). Observed and anticipated impacts of drought on forest insects and diseases in the United States. *Forest Ecology and Management*, *380*, 321–334. https://doi.org/10.1016/j.foreco.2016.04.051

McCabe, G. J., & Markstrom, S. L. (2007). A Monthly Water-Balance Model Driven By a Graphical User Interface. *U.S . Geological Survey*, 1–12.

McCabe, G. J., & Wolock, D. M. (2008). Joint Variability of Global Runoff and Global Sea Surface Temperatures. *Journal of Hydrometeorology*, *9*(4), 816–824. https://doi.org/10.1175/2008jhm943.1

McMillan, S. K., Wilson, H. F., Tague, C. L., Hanes, D. M., Inamdar, S., Karwan, D. L., Loecke, T., Morrison, J., Murphy, S. F., & Vidon, P. (2018). Before the storm: antecedent conditions as regulators of hydrologic and biogeochemical response to extreme climate events. *Biogeochemistry*, *141*(3), 487–501. https://doi.org/10.1007/s10533-018-0482-6

Moeser, D., & Douglas-Mankin, K. (2017). Hydrologic Impacts of Wildfire on a Small Sub-alpine Southwestern U.S. Watershed: A Simplified Modeling Approach. *American Geophysical Union, Fall Meeting*. https://ui.adsabs.harvard.edu/abs/2017AGUFM.H21B1448M/abstract

Myneni, R., Knyazikhin, Y., & Park, T. (2015). *MCD15A3H MODIS/Terra+Aqua Leaf Area Index/FPAR 4-day L4 Global 500m SIN Grid V006*. NASA EOSDIS Land Processes DAAC. https://doi.org/10.5067/MODIS/MCD15A3H.006

Nash, E., & Sutcliffe, V. (1970). River flow forecasting through conceptual models Part 1 - A discussion of principles. *Journal of Hydrology*, *10*, 282–290.

Parker, T. J., Clancy, K. M., & Mathiasen, R. L. (2006). Interactions among fire, insects and pathogens in coniferous forests of the interior western United States and Canada. *Agricultural and Forest Entomology*, *8*(3), 167–189. https://doi.org/10.1111/j.1461-9563.2006.00305.x

Penn, C. A., Clow, D. W., Sexstone, G. A., & Murphy, S. F. (2020). Changes in Climate and Land Cover Affect Seasonal Streamflow Forecasts in the Rio Grande Headwaters. *Journal of the American Water Resources Association*, *56*(5), 882–902. https://doi.org/10.1111/1752-1688.12863

PRISM. (2020). *PRISM Climate Group, Oregon State University*. http://prism.oregonstate.edu/

Regan, R. S., Juracek, K. E., Hay, L. E., Markstrom, S. L., Viger, R. J., Driscoll, J. M., LaFontaine, J. H., & Norton, P. A. (2019). The U. S. Geological Survey National Hydrologic Model infrastructure: Rationale, description, and application of a watershed-scale model for the conterminous United States. *Environmental Modelling and Software*, *111*(September 2018), 192–203. https://doi.org/10.1016/j.envsoft.2018.09.023

Rood, S. B., Pan, J., Gill, K. M., Franks, C. G., Samuelson, G. M., & Shepherd, A. (2008). Declining summer flows of Rocky Mountain rivers: Changing seasonal hydrology and probable impacts on floodplain forests. *Journal of Hydrology*, *349*(3–4), 397–410. https://doi.org/10.1016/j.jhydrol.2007.11.012

Running, S., Mu, Q., & Zhao, M. (2017). *MOD16A2 MODIS/Terra Net Evapotranspiration 8-Day L4 Global 500m SIN Grid V006 [Data set]*. NASA EOSDIS Land Processes DAAC.

Rust, A. J., Randell, J., Todd, A. S., & Hogue, T. S. (2019). Wildfire impacts on water quality, macroinvertebrate, and trout populations in the Upper Rio Grande. *Forest Ecology and Management*, *453*(February). https://doi.org/10.1016/j.foreco.2019.117636

Saxe, S., Hogue, T. S., & Hay, L. (2018). Characterization and evaluation of controls on post-fire streamflow response across western US watersheds. *Hydrology and Earth System Sciences*, *22*(2), 1221–1237. https://doi.org/10.5194/hess-22-1221-2018

Schneider, K.E., Rust, A., Randell, J., Hogue, T.S. Evaluating Hydrologic Impact from Concurrent Insect and Fire Disturbances. *Journal of Hydrology: Regional Studies,* (in-review)

Sexstone, G. A., Penn, C. A., Liston, G. E., Gleason, K. E., Moeser, C. D., & Clow, D. W. (2020).

Spatial variability in seasonal snowpack trends across the rio grande headwaters (1984–2017). *Journal of Hydrometeorology*, *21*(11), 2713–2733. https://doi.org/10.1175/JHM-D-20-0077.1

Silins, U., Stone, M., Emelko, M. B., & Bladon, K. D. (2009). Sediment production following severe wildfire and post-fire salvage logging in the Rocky Mountain headwaters of the Oldman River Basin, Alberta. *Catena*, *79*(3), 189–197. https://doi.org/10.1016/j.catena.2009.04.001

Stephens, S. L., Collins, B. M., Fettig, C. J., Finney, M. A., Hoffman, C. M., Knapp, E. E., North, M. P., Safford, H., & Wayman, R. B. (2018). Drought, Tree Mortality, and Wildfire in Forests Adapted to Frequent Fire. *BioScience*, *68*(2), 77–88. https://doi.org/10.1093/biosci/bix146

Stevens-Rumann, C. S., & Morgan, P. (2019). Tree regeneration following wildfires in the western US: a review. *Fire Ecology*, *15*(1), 1–17. https://doi.org/10.1186/s42408-019-0032-1

Temperli, C., Bugmann, H., & Elkin, C. (2013). Cross-scale interactions among bark beetles , climate change , and wind disturbances : a landscape modeling approach. *Ecological Monographs*, *83*(3), 383–402.

US Environmental Protection Agency. (2012). *Level IV Ecoregions of Colorado*. U.S. EPA Office of Research and Development (ORD) - National Health and Environmental Effects Research Laboratory (NHEERL). https://gaftp.epa.gov/EPADataCommons/ORD/Ecoregions/co/co_eco_l4.htm

Westerling, A. L. (2006). Warming and Earlier Spring Increase Western U.S. Forest Wildfire Activity. *Science*, *313*(5789), 940–943. https://doi.org/10.1126/science.1128834

Wlostowski, A. N. (2019). *Analysis and Technical Updates to the Colorado Water Plan: Technical Memorandum*.

Zambrano-Bigiarini, M. (2020). *hydroGOF: Goodness-of-fit functions for comparison of*

simulated and observed hydrological time series (R package version 0.4-0). https://doi.org/10.5281/zenodo.839854
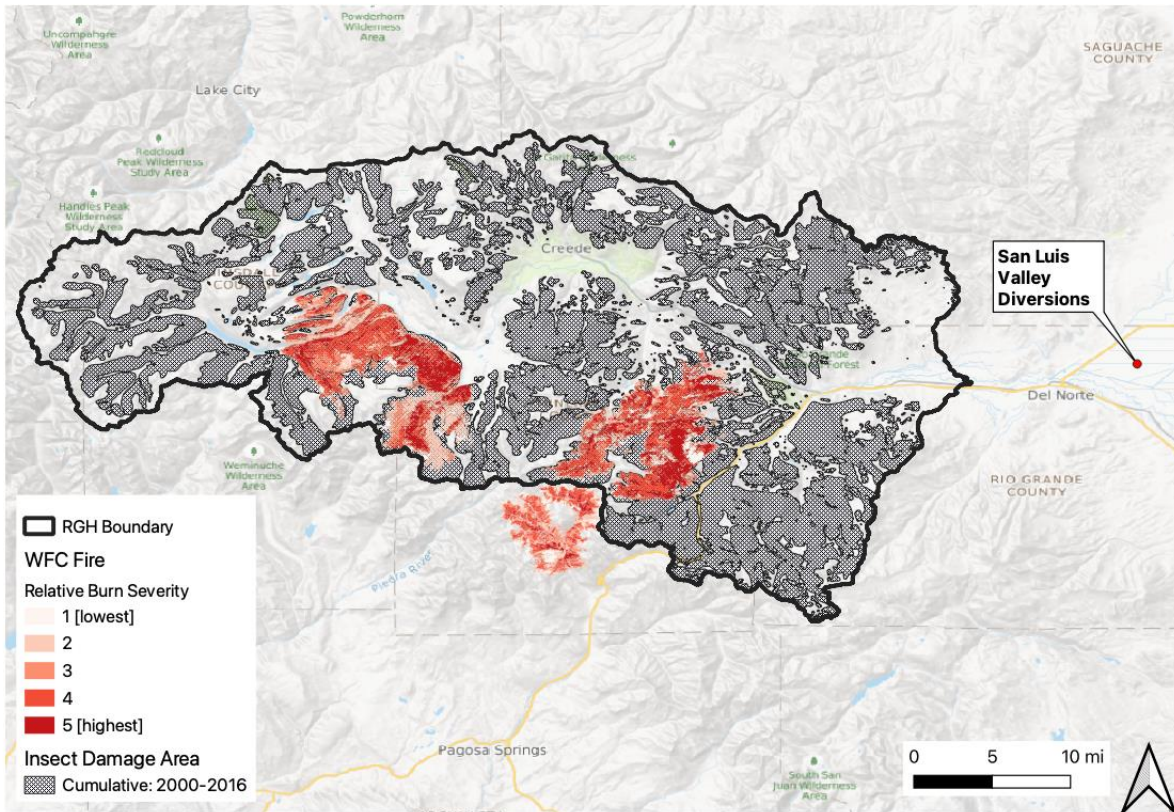
Appendix

Figure A1- Map of recent disturbances in the Rio Grande Headwaters

Table A1 – Model Parameterization, Calibration & Validation Summary

Calibration Parameter		Original MWBM [baseline]	MWBM-LAI [baseline]	MWBM-LAI [fire-scenario]
Original Calibration Parameters	Tsnow	-0.7	-0.7	-0.32
	Train	1.81	1.81	1.21
	drofrac	0.31	0.31	0.03
	meltmax	0.71	0.71	0.53
	STC	1112	1112	90
	rfactor	0.49	0.49	0.35
Pfactors	Winter	1.34	1.34	1.34
	Spring	0.7	0.7	0.7
	Summer	0.16	0.16	0.16
	Fall	0.8	0.8	0.8
Model Period	Objective Function	Objective Function Value		
Calibration Period	*WY 07-09 Oct 2006 - Sept 2009*	NSE	0.78	0.77	--
		PBIAS	-3	0.3	--
		50/50 Score	87.27	88.21	--
Validation Period	*WY 10-12 Oct 2009 - Sept 2012*	NSE	0.7	0.65	--
		PBIAS	-1.2	9.1	--
		50/50 Score	84.41	78.07	--
Post-fire Evaluation Period	*June 2013 - Dec 2017*	NSE	0.56	0.64	0.72
		PBIAS	-40.8	-31.4	-1.3
		50/50 Score	57.81	66.43	85.34

Table A2- Decadal Absolute Values of RO by Scenario

		Runoff Absolute Values [mm]					
	Decade	Baseline	Climate Only	Forest Change + Climate	Fire 2041 Only	Fire 2041 + Climate	Fire 2031 + Climate
Average Annual Runoff Total	2021-30	166.06	162.15	162.15	166.06	162.15	162.15
	2031-40	169.16	154.79	154.79	169.16	154.79	216.25
	2041-50	169.19	145.24	145.24	223.28	209.65	203.78
Average Melt Season Runoff Total [Apr - Jun]	2021-30	33.5	33.75	33.75	33.5	33.75	33.75
	2031-40	33.68	32.46	32.46	33.68	32.46	41.90
	2041-50	33.68	30.3	30.3	39.44	40.37	40.19
Average Monsoon Season Runoff Total [Jul - Sept]	2021-30	14.95	13.33	13.33	14.95	13.33	13.33
	2031-40	14.97	11.05	11.05	14.97	11.05	22.27
	2041-50	14.97	9.15	9.15	27.12	17.4	17.10
Average Low-Flow Runoff Total [Oct - Dec]	2021-30	5.33	5.32	5.32	5.33	5.32	5.32
	2031-40	5.34	5.4	5.4	5.34	5.4	7.82
	2041-50	5.34	5.66	5.66	9.92	6.46	5.54
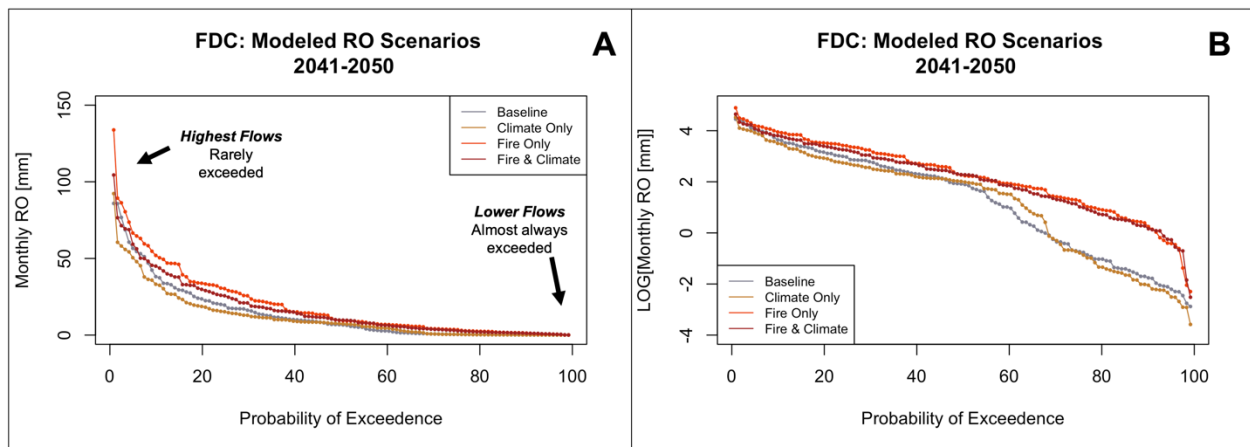
Figure A2- Flow duration curves for the last simulation decade.
Each dot represents a month of simulated RO. A) axes are untransformed. B) y-axis is log-transformed for ease of viewing low RO values.

- Here, changes in flow magnitudes for the last decade is through flow duration curves (FDCs) (**Figure A2**). FDCs reveal differences in scenario RO over a more-continuous range of flow magnitudes. Low flows have a higher probability of exceedance, while higher flows have a low probability of exceedance. Simulated RO trends in FDCs agree with trends in RO quartiles; "Climate Only" RO is always lower than baseline RO (except for during more moderate flow), and fire scenario RO is always higher than baseline. Differences in low flows are particularly evident in FDCs which illustrate the stark difference between fire-scenarios and non-fire scenarios (including baseline).